MEASURE AND SIMULATION OF THE EFFECT OF MATRIX DAMAGE ON COMPRESSIVE STRENGTH IN THE FIBER DIRECTION OF CFRP

Olivier Montagnier[1], Christian Hochard[2], Aldo Cocchi[2] and Gabriel Eyer[2]

[1]Centre de Recherche de l'Armée de l'air (CReA), Ecole de l'air, BA 701, 13361 Salon air, France
Email: olivier.montagnier@ecole-air.fr, Web Page: http://www.crea.defense.gouv.fr
[2]Aix Marseille Univ., CNRS, Centrale Marseille, LMA, Marseille, France
Email: hochard@lma.cnrs-mrs.fr, Web Page: http://www.lma.cnrs-mrs.fr/

Keywords: compression - experimental - carbon/epoxy - damage - continuum damage mechanics.

Abstract
The influence of transverse damage on compressive strength in fiber direction for carbon fiber reinforced epoxy materials is investigated by an experimental approach. Two experimental methods are proposed. The first study focuses on tubular samples. Theses samples are damaged by cyclic torsional load and next submitted to a compressive load up to failure. Results show that the transverse damage affects drastically the compressive strength. Yet the stiffness is not modified. A model is then proposed with these results. In the second part, the idea is to generate compression in the fiber direction in a ply of a laminate through adjacent plies. The proposed laminate is a [45/-45/90/-45/45] laminate subject to tension. By a "scissors effect" of the ±45° plies, the 90° ply is loaded in compression, and secondly, strongly damaged by transverse stress. Experiments seems to be able to say that failure of this laminate is due to compression. Simulation of these experiments with the model proposed and implemented in ABAQUS seems also to confirm these results.

1. Introduction

The composite materials behavior in compression is complex and is still poorly known today. The difficulties for this kind of loading case is related in both experimental measurement and modeling. The phenomenon of failure seems well observed at the micro scale (fiber micro-buckling) but the link between modeling at this scale and experimental results (at the macro scale) remains complex. In general, experimental studies are still limited and focus rarely on the impact of damage on compressive strength. The aim of this work is therefore to fill this gap and to deals with the influence of matrix damage on the compressive strength in the fiber direction of carbon/epoxy composites.

It was demonstrated that transverse damage causes a drop of the tensile strength in [1]. This drop is only visible for high damage ($d > 0.8$). Similarly, it can be assumed that compression strength will be affected by transverse damage. When the matrix is completely destroyed, the slenderness of the fibers leads to instantaneous micro-buckling or more globally to the catastrophic failure of the laminate. Researches show that the increase of temperature (which causes matrix damage) leads to the progressive reduction of compressive strength for glass/polypropylene composites [2].

In this work, a model based on the damage mechanics [3] already developed in shear and tension for static and fatigue cases [1], is adapted here to the case of compression thanks to the experimental results. Two kind of experimental tests are proposed here. The first one is a homogeneous test of compression on woven carbon/epoxy tubes, previously damaged with a cyclic torsional load. The second test is a tensile test on a laminate [45, -45,90, -45,45]. These make it possible to apply compression in the fiber direction of 90° plies, strongly damaged by the transverse stress.

2. Continuum damage mechanics of a ply

The model proposed is based on Continuum Damage Mechanics (CDM). It describes directly the mechanical behavior of the composite material on the ply scale (meso-model). The processes occurring at the micro-scale are described via thermodynamic expressions.

2.1. Damage behavior of UD ply

The damage is only considered in the plane of the ply and assumed to be uniform throughout the thickness of the ply. It is expressed in terms of loss of stiffness:

$$E_1 = E_1^0 (1 - d_1) \; ; \; E_2 = E_2^0 (1 - d_2) \; ; \; G_{12} = G_{12}^0 (1 - d_{12}) \quad \text{with} \quad \{d_1, d_2, d_{12}\} \in [0, 1] \tag{1}$$

where d_1, d_2 and d_{12} are the damage in axial, in transverse and in shear directions, respectively. These damage variables are initially null then E_1^0, E_2^0 and G_{12}^0 are initial stiffness in axial, in transverse and in shear directions, respectively. Assuming that we are dealing with plane stresses and small perturbations assumptions, the local strain energy of each ply can be written in terms of stresses as follows [3]:

$$E = \frac{1}{2} \left(\frac{\langle \sigma_1 \rangle_+^2}{E_1^0 (1 - d_1)} + \frac{\langle \sigma_1 \rangle_-^2}{E_1^0} + \frac{\langle \sigma_2 \rangle_+^2}{E_2^0 (1 - d_2)} + \frac{\langle \sigma_2 \rangle_-^2}{E_2^0} - 2 \frac{\nu_{12}^0}{E_1^0} \sigma_1 \sigma_2 + \frac{\sigma_{12}^2}{G_{12}^0 (1 - d_{12})} \right) \tag{2}$$

where $\langle . \rangle_+$ and $\langle . \rangle_-$ stand for positive part and negative part. Noting that there is no damage during compressive steps. Thermodynamic forces associated to internal variables can be deduced from strain energy:

$$Y_{d_j} = \frac{\partial E}{\partial d_j} = \frac{\langle \sigma_j \rangle_+^2}{2 E_j^0 \left(1 - d_j\right)^2} \quad j \in \{1, 2\} \; ; \quad Y_{d_{12}} = \frac{\partial E}{\partial d_{12}} = \frac{\sigma_{12}^2}{2 G_{12}^0 (1 - d_{12})^2} \tag{3}$$

The development of internal variables depends on these thermodynamic forces or more specifically, on their maximum values during the loading history. In the fiber direction, the brittle fracture is described with a threshold model:

$$d_1 = 0 \quad \text{if} \quad Y_{d_1} < Y_{d_1}^{\max} \quad \text{else} \quad d_1 = 1 \tag{4}$$

The damage in the transverse direction is based on a statistic law [4]:

$$d_2 = \left\langle 1 - e^{-(Y_{eq} - Y_0)} \right\rangle_+ \quad \text{with} \quad \dot{d_2} \geq 0 \tag{5}$$

where $Y_{eq} = a Y_{d_2}^m + b Y_{d_{12}}^n$ is an equivalent thermodynamic force that accounted for the coupling mechanism between damage in transverse and shear direction. The damage mechanisms like matrix micro-cracking decrease the transverse and shear stiffness at the same time. Accordingly, the damage in shear direction is assumed to be proportional to the previous one:

$$d_{12} = c d_2 \tag{6}$$

2.2. Inelastic strain of UD ply

Inelastic strains were observed in case of $[45]_8$ laminate in [4]. Here, only the inelastic strains in the shear direction is taken into account. The coupling between damage and plasticity is accounted for in terms of the effective stress and the effective strain [3]:

$$\tilde{\sigma}_{12} = \frac{\sigma_{12}}{1 - d_{12}} \quad \text{and} \quad \dot{\tilde{\varepsilon}}_{12}^p = \dot{\varepsilon}_{12}^p (1 - d_{12}) \tag{7}$$

A kinematic linear hardening model is used to describe these strains where it is assumed that the stresses σ_1 and σ_2 has no effect:

$$f = \left| \tilde{\sigma}_{12} - C_0 \tilde{\varepsilon}_{12}^p \right| - R_0 \tag{8}$$

where R_0 is the initial inelastic strain threshold and C_0 is the linear law coefficient. Then, evolution of plastic strains exists when $f > 0$.

Olivier Montagnier, Christian Hochard, Aldo Cocchi and Gabriel Eyer

3. Composite tubes: fatigue damage and compression up to failure

The aim of this part is to propose an experimental method that would make it possible to damage the matrix of a composite as well as achieve compression in the fiber direction. Two approaches are possible: one consisting in providing one single experimental setup for both steps and the other consisting in providing one experimental setup for each step. Here we have chosen the second one. This is possible with composite tubes constituted of fibers aligned with the tube axis and loaded in torsion and in compression (Fig. 1a). The cyclic torsional load is used to damage the matrix in shear whereas the static compression load is applied in a second phase up to rupture to quantified the ultimate stress.

It is well known that pure compression test are particularly complex to perform on unidirectional composite specimen because of the risk of buckling and large stress concentration at the tabs. A large literature can be found about these issues [5]. Here, in order to limit these difficulties, it is proposed to used a dumbbell-shaped tube geometry, a large thickness for the gauge, a woven material, and a softer material for the tabs ([90°] plies of unbalanced woven glass/epoxy). A careful development of this test is proposed in [6, 7, 8, 9].

3.1. Experimental protocol

Tubes are manufactured in two steps (Fig. 1a). First, a tube made of balanced woven carbon/epoxy (G939/M18 Table 1) is manufactured using a wrap rolling process around an aluminum rod. A heat-shrinkable tape is used to ensure compaction during curing. The thermal coefficient of aluminum being greater than that of the composite, allows the aluminum rod to be removed after the curing cycle. The stacking sequence of the tube is $[0°]_{11}$ and the thickness is equal to 2.75 mm in order to avoid buckling. Next, the carbon tube is reinforced with tabs at both ends.
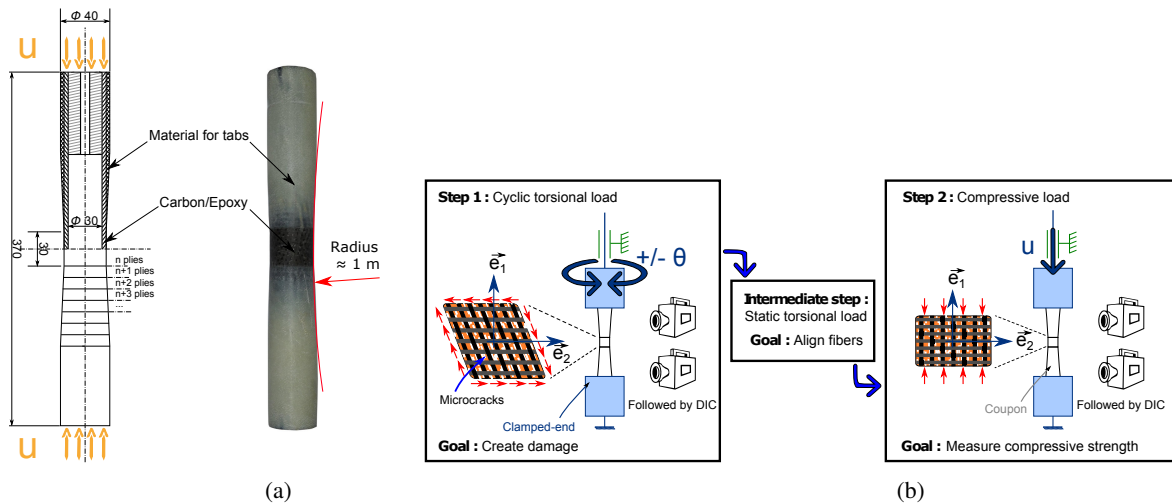

Figure 1. A method to apply fatigue damage and compression up to rupture on a composite tube : (a) geometry of the tube sample, (b) illustration of the different steps of the experiment

The test is performed on a axial-torsion universal testing machine and followed by 3D Digital Image Correlation (DIC). Figure 1b gives a description of the 3-step protocol. In the first step, torsion is applied to the tube specimen in order to shear the matrix and thus, to create diffuse damage. In the case of carbon/epoxy woven plies it is not possible to create damage of more than 0.5 with a static load because the stiffness reduction leads to material instability [3]. That is why it is necessary to use a cyclic load. The damage is measured after each step of 500 cycles. When the value of damage is considered to be enough, an intermediate step is to realign the fibers in the gauge area along the compression load direction by using DIC. Finally, the compressive test is performed up to rupture.

Olivier Montagnier, Christian Hochard, Aldo Cocchi and Gabriel Eyer

Table 1. Properties of the woven carbon/epoxy material G939/M18

E_1^0	E_2^0	G_{12}^0	ν_{12}	a	b	c	m	n	Y_0	C_0	R_0	σ_t	$\sigma_c^{d=0}$	γ	t
GPa	GPa	GPa	-	MPa^{-m}	MPa^{-n}	-	-	-	-	MPa	MPa	MPa	MPa	-	mm
53	53	3.8	0.035	0.7	0.25	1	0.75	0.75	0	6500	50	820	590	12	0.26

3.2. Test on undamaged specimens

Undamaged specimens are first studied [8]. Fig. 2a shows the longitudinal strain field of an undamaged tube just before failure. The strain is not perfectly uniform in the gauge area and the tab reinforcements affect slightly the strain field. That is why an average strain is computed to obtain the experimental σ-ε curve (Fig. 2b). The collapse is obtain for $\varepsilon_c^{d=0}$ = 1.35 % which is close to the ultimate tensile strain ($\varepsilon_t^{d=0}$ = 1.5 % [10]), but the ultimate stress is different in traction and in compression (see Table 1) because the behavior is significantly non linear. The model proposed by Allix *et al.* in [11] is used here in order to model this non linear behavior:

$$\sigma = E_1^0(1 + \gamma\varepsilon)\varepsilon \qquad (9)$$

The identified curve is plotted in Fig. 2b for γ = 12. The curve shows a good agreement with the experimental data.
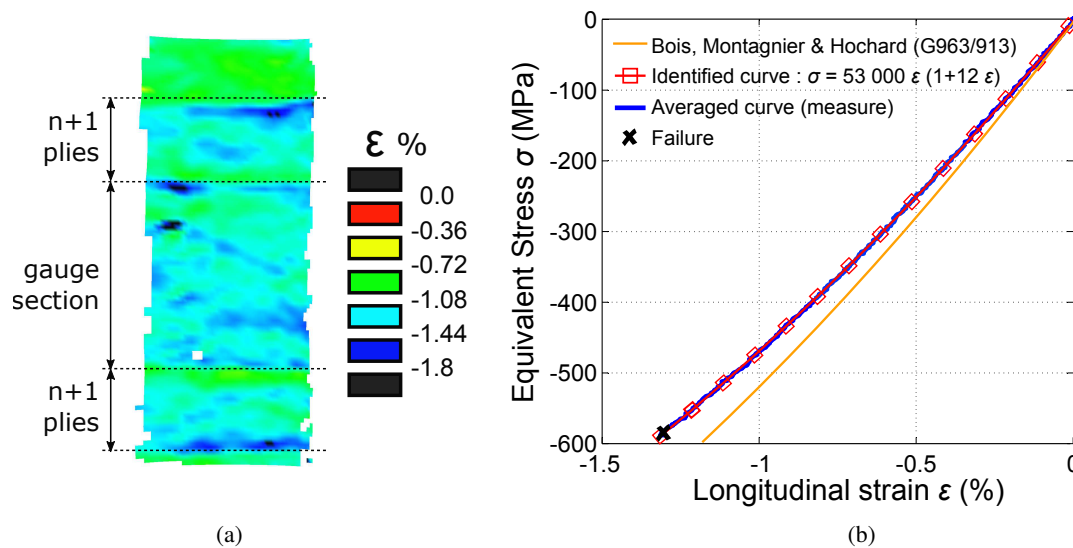

Figure 2. Compression of an undamaged tube: (a) strain field in tube direction just before collapse, (b) non linear behavior in compression up to failure (woven carbon/epoxy material G939/M18)

3.3. Test on damaged specimens

The effect of transverse damage is now studied using the full experimental protocol described above. After cyclic torsional load, a full torsion cycle at low speed permits to identify the level of damage. Figure 3a shows these cycles for two different tubes in comparison with the initial behavior. The measurement of the cycle slope gives directly the damage parameter with the relation $d_{12} = 1 - G_{12}^d/G_{12}^0$. Moreover, because the parameter c of the CDM model is particularly complex to identify experimentally, it is assumed that $d_2 = d_{12} = d$ (corresponding to the case c = 1).

Fig. 3b represents the compressive behavior in fiber direction for different damaged tubes. It can be observed that the non linear behavior identified in the previous section is not affected by the level of tube damage because is directly linked to fiber stiffness not affected by these damage. On the other hand, the
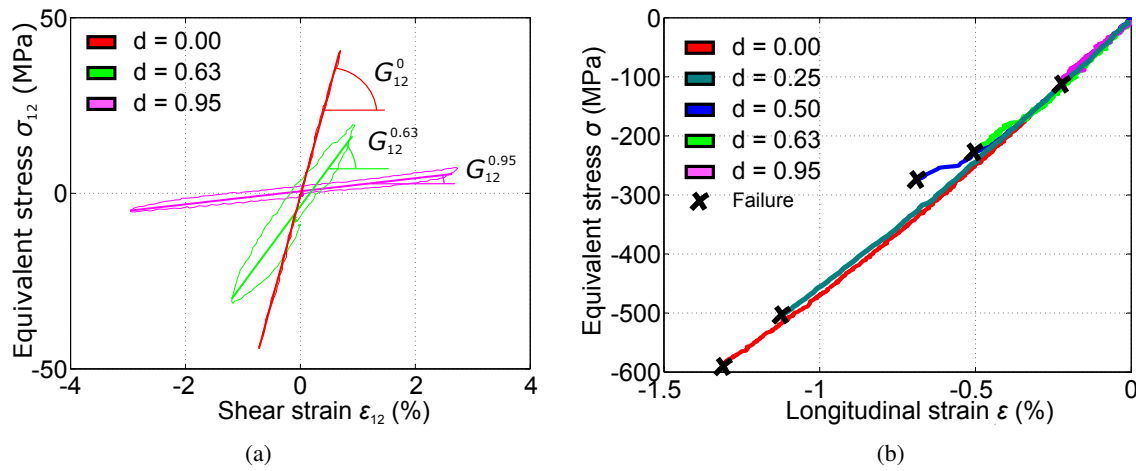
Olivier Montagnier, Christian Hochard, Aldo Cocchi and Gabriel Eyer

Figure 3. Experimental test results on tubes: (a) Shear behavior for the last torsion cycle at low speed used to the loss of rigidity (*d*) for three different specimens (a) Compression behavior for different damage states (woven carbon/epoxy material G939/M18)
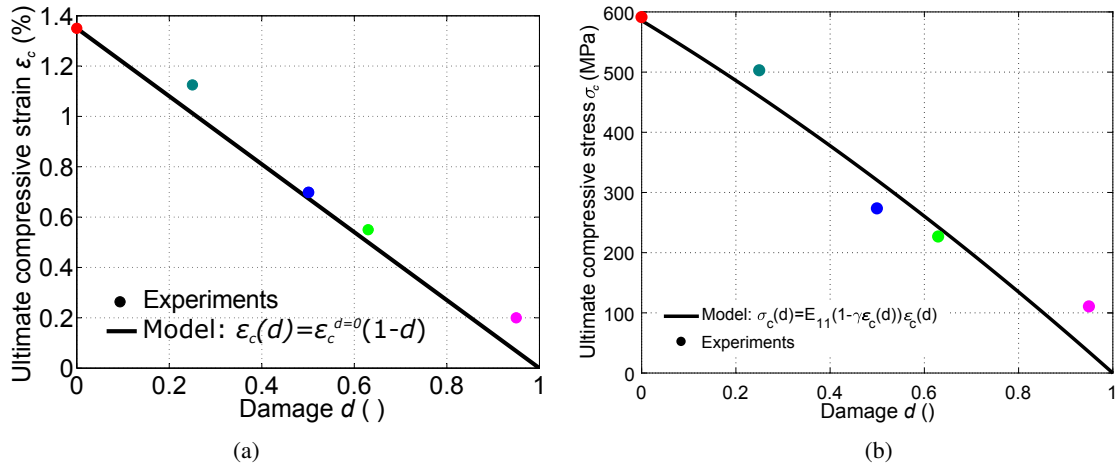

Figure 4. Effect of matrix damage on compressive failure in the fiber direction: (a) ultimate compressive strain, (b) ultimate compressive stress (woven carbon/epoxy material G939/M18)

ultimate stress and strain at failure are drastically affected by the level of damage because compressive failure (kinking instability) is directly linked to the matrix shear behavior [12, 13].

In Fig. 4, the strain and the stress leading to failure is plotted according to the damage. A linear decrease in the ultimate compressive strain is observed when the value of damage increases. To take this strength reduction in calculations, a simple linear model is proposed as follows:

$$\varepsilon_c^d = \varepsilon_c^{d=0}(1 - d) \tag{10}$$

which gives a non linear criteria for the ultimate stress according to Eq. 9:

$$\sigma_c^d = E_1^0(1 + \gamma \varepsilon_c^d)\varepsilon_c^d \tag{11}$$

These laws (Eqs (9) & (11)) are implemented in ABAQUS via a Umat procedure previously developed in [14, 1].

Olivier Montagnier, Christian Hochard, Aldo Cocchi and Gabriel Eyer

4. Tensile test on [45,-45,90,-45,45] laminate leading to 90° ply compressive failure

In this last part, the objective is to show the interest of the previous results (Eq. 11) on a particular laminate. The idea is to generate compression in the fiber direction of a ply in a laminate via adjacent plies [15, 16]. The test proposed here is a laminate [45/-45/90/-45/45] in tension. By a "scissors effect" of the plies [45/-45] in tension, the 90° ply is subject to compression. This consequence can be also explained by Poisson effect. On the other hand, the tension of the laminate involves a longitudinal strain of the laminate and consequently a transverse strain of the 90° ply. This strain lead implicitly to transverse damage ($d_2 = d$) which can influence the compression failure. Finally, this test could be considered as an original test of compression but with an imposed transverse strain.

Here, the studied material is unidirectional carbon/epoxy T700GC/M10 (Table 2). For this material, ultimate compression strain is of the order of $\varepsilon_c^{d=0} = 1.5$ %. If the 90° ply of the laminate breaks first by compression, it can be assumed that it will be for this level of strain. In fact, it is not reasonable to assume that there is no effect of transverse strain. An ABAQUS simulation of the laminate with the model proposed above predicts a failure of the 90° ply for a strain of only $\varepsilon_c^d = 0.65$ % corresponding to a high level of damage. At this step, the simulation gives a axial strain of the laminate of 1.45 %.

Table 2. Properties of the unidirectional carbon/epoxy material T700GC/M10

E_1^0	E_2^0	G_{12}^0	v_{12}	a	b	c	m	n	Y_0	C_0	R_0	σ_t	$\sigma_c^{d=0}$	γ	t
GPa	GPa	GPa	-	MPa^{-m}	MPa^{-n}	-	-	-	-	MPa	MPa	MPa	MPa	-	mm
110	7.5	3.9	0.3	1	0.55	1	0.65	0.6	0	8500	55	2314	1500	15	0.26

The first test is performed on a dumbbell-shaped test specimen with very large radii of curvature (1 m), which makes it possible to obtain a homogeneous strain field in the gauge area of the specimen. The homogeneity of the field is clearly visible in the first part of the curve shown in Fig. 5. The solid curve represents the strain in the direction of the specimen ($\vec{y}$) i.e. in the transverse direction of the 90° ply. The dotted line represents the strain in the direction perpendicular to the sample ($\vec{x}$) i.e. the fiber direction of the 90° ply. The curve very distinctly presents two zones. A first zone up to point C and a second between points C and D. It is also noted that the force-displacement curve has a sudden drop in the force at point C. Moreover it appears that after this point the strain in the transverse direction increases largely. This corresponds to an increase in the Poisson's ratio. One hypothesis is that the 90° fibers broke at the point C. Indeed, if these fibers are broken, the Poisson's ratio (at the scale of the laminate) is no longer blocked. This translates into an increase in this coefficient. The axial strain at failure for the laminate is very close to the expected value at point C (i.e. 1.6%). Finally some post mortem micrographs, tend to show the presence of kink-band. It is therefore probable that the rupture of the fibers at 90 ° (in compression) may be the cause of the failure of the laminate. It remains to be shown that delamination is not the cause of the failure.

One technique to rule out the delamination of possible causes of failure is to modify the free edges. Thus, it is proposed to reinforce the lateral edges of the test specimen with epoxy resin (reinforced with glass micro-balls) and to measure the ultimate strain again (sample 2). It appears that the behavior is not significantly affected (Fig. 6), which makes it possible to assume that the failure of the 90° ply in compression is the cause of the rupture. The comparison of the two tests and the simulation is also given in Fig. 6. It shows a good prediction of the behavior and the compression rupture of the ply at 90 ° at the same time justifying the proposed model.

5. Conclusion

In conclusion, the strong influence of matrix damage on the compressive strength in fiber direction of laminated composites is experimentally demonstrated from two kind of tests. The first one is a homogeneous compression test of woven tubes previously damaged with torsional cyclic load. This test is complex to perform but allows to establish a mesoscale model based on a damage variable to describe
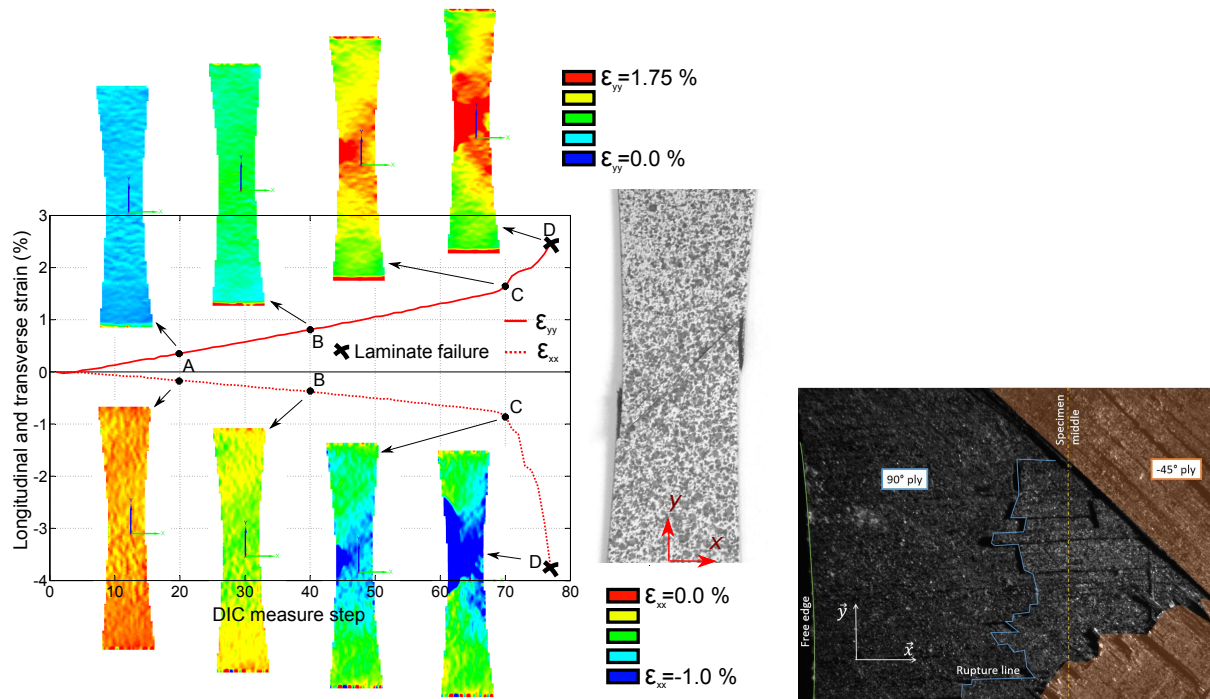
Olivier Montagnier, Christian Hochard, Aldo Cocchi and Gabriel Eyer

Figure 5. Strains evolution in the tensile test of a laminate [45,-45,90,-45,45] (along the direction $\vec{y}$) and visualization of the rupture line in the 90° ply after manual peeling of ±45° plies.
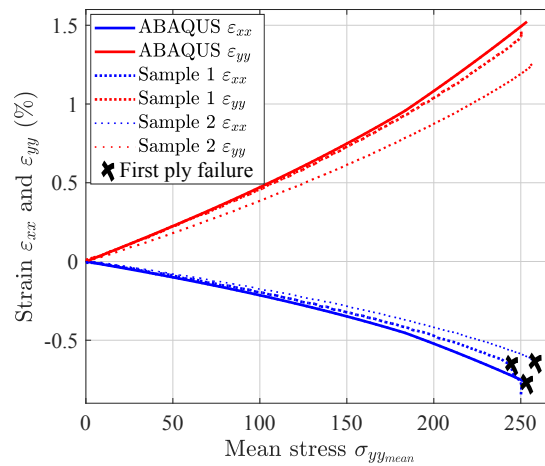

Figure 6. Stress/strain curve of a laminate [45,-45,90,-45,45] in tension along the direction $\vec{y}$: experiments versus simulation.

the decrease of the ultimate compressive stress. In the second test, the model is used to predict the failure of the laminate [45, -45,90, -45,45] in tension. These laminates make it possible to apply an homogeneous compression to the 90° ply in the fiber direction, but also to strongly damage it by transverse stresses. The proposed model and the experiments carried out seem to be able to explain the failure of these laminates by compression failure of the 90° ply.

Acknowledgments

Olivier Montagnier, Christian Hochard, Aldo Cocchi and Gabriel Eyer

References

[1] C Hochard, S Miot, Y Thollon, N Lahellec, and J-P Charles. Fatigue of laminated composite structures with stress concentrations. *Composites Part B: Engineering*, 65:11–16, 2014.

[2] A.G. Gibson, M.E. Otheguy Torres, T.N.A. Browne, S. Feih, and A.P. Mouritz. High temperature and fire behaviour of continuous glass fibre/polypropylene laminates. *Composites Part A: Applied Science and Manufacturing*, 41(9):1219–1231, September 2010.

[3] P. Ladevèze and E. Le Dantec. Damage modelling of the elementary ply for laminated composites. *Composites Science and Technology*, 43(3):257–267, 1992.

[4] Y Thollon and Ch Hochard. A general damage model for woven fabric composite laminates up to first failure. *Mechanics of Materials*, 41(7):820–827, 2009.

[5] D Adams. Current compression test methods. *High-Performance Composites*, 3:40–41, may 2005.

[6] G. Eyer. *Rupture des matériaux composites en compression sens fibre. Analyse de l'effet de l'endommagement.* PhD thesis, Université d'Aix-Marseille, 2015.

[7] G. Eyer, O. Montagnier, J-P. Charles, and C. Hochard. Effect of transverse damage on compressive strength in fiber direction for cfrp. In *ECCM Seville*, 2014.

[8] G Eyer, O Montagnier, J-P Charles, and C Hochard. Design of a composite tube to analyze the compressive behavior of cfrp. *Composites Part A: Applied Science and Manufacturing*, 87:115–122, 2016.

[9] G Eyer, O Montagnier, C Hochard, and J-P Charles. Effect of matrix damage on compressive strength in the fiber direction for laminated composites. *Composites Part A: Applied Science and Manufacturing*, 94:86–92, 2017.

[10] C. Bois, O. Montagnier, and C. Hochard. Caractérisation du comportement en compression des matériaux composites par essais de flexion pure. In *15eme Journées Nationales des composites*, pages 107–114, 2007.

[11] O. Allix, P. Ladeveze, and E. Vittecoq. Modelling and identification of the mechanical behaviour of composite laminates in compression. *Composites science and technology*, 51(1):35–42, 1994.

[12] B. W. Rosen. Mechanics of composite strenghtening. in fibre composite materials. *American Society for metals*, pages 37–75, 1964.

[13] B. Budiansky and N. A. Fleck. Compressive failure of fibre composites. *Journal of the Mechanics and Physics of Solids*, 41(1):183–211, 1993.

[14] Christian Hochard, Noël Lahellec, and Cyril Bordreuil. A ply scale non-local fibre rupture criterion for cfrp woven ply laminated structures. *Composite Structures*, 80(3):321–326, 2007.

[15] O. Montagnier, G. Eyer, and Ch. Hochard. Effet de l'endommagement de la matrice sur la rupture en compression sens fibre des composites. In *Journées Nationales sur les Composites 2017*, 2017.

[16] F. Laurin, P. Paulmier, and F.-X. Irisarri. Détermination de la résistance de compression longitudinale d'un pli ud carbone/epoxy à partir d'un essai de traction sur stratifié. In *Journées Nationales sur les Composites 2017*, 2017.